

NATURAL LAMINAR FLOW DESIGN OF FUSELAGE NOSE FOR SMALL SUPERSONIC CIVIL TRANSPORT

Naoko TOKUGAWA¹, Tae OSADA², Yoshine UEDA³ and Hiroaki ISHIKAWA⁴
¹Japan Aerospace Exploration Agency, ²Gakushuin University,
³Tokyo Business Service Co. Ltd., ⁴TOUA Co. Ltd.

Keywords: *Boundary layer transition, Cross-flow instability, Numerical Prediction, Shape modification*

Abstract

A natural laminar flow fuselage nose was designed numerically at scale and with a Reynolds number corresponding to the small supersonic civil transport QSST aimed to reduce friction drag. The natural laminar flow effect was evaluated using the transition analysis for the parametric modified fuselage nose from the baseline shape. As a result, the transition front, which is predicted as the contour corresponding to $N = 14$, moved 2 m further downstream from the nose tip for the cases based on Sears-Haack body. On the other hand, slight deformation was applied for the cases based on QSST, preventing the flow from the windward side to the leeward side. A decrease of large cross-flow velocity was observed along with the resultant delay of transition front.

1 Introduction

One decade has already passed since the retirement of the dream supersonic transport *Concorde*. Nevertheless, no successor transport has been developed or operated. The key reasons for this are the same reasons why *Concorde* was the so-called commercial flop: its deafening sonic-boom and poor fuel efficiency. The Japan Aerospace Exploration Agency (JAXA) has been addressing these two technical issues toward development of a next-generation supersonic transport. To mitigate the sonic boom, a low-boom airframe has been designed and is going to be validated by the drop test through the on-going *D-SEND* project [1, 2]. On the other hand, in order to improve fuel

efficiency, four concepts were applied to the non-powered supersonic experimental airplane *NEXST-1*. Those are the arrow planform, the area-rule fuselage, the warp-design, and the world's first subsonic leading-edge natural laminar flow (NLF) wing. Furthermore, its efficiency was evaluated through a flight test [3, 4]. This reduction of drag, especially the reduction of friction drag, is an enduring technical issue, not only of *NEXST-1* but also of all transport. Therefore many approaches have been invented and examined [5-19]. Throughout those investigations, the NLF technology is apparently being evaluated as effective technology with minimum cost.

As represented by *NEXST-1*, attention has been focused on the wing, but not on the fuselage nose because of its small wetted-area size [11-13]. Moreover, many earlier studies have examined the boundary layer transition related to nose-like shapes in supersonic flows, emphasizing the transition mechanism or the nature of disturbance growth [20-25]. In other words, proposals for NLF fuselage nose are rare. However, demands on increased fuel efficiency are growing daily [9, 10]. Some room for small improvement cannot be neglected. Those demands raise our motivation to design a superior NLF fuselage nose.

Recently, the present authors have produced an NLF fuselage nose design concept for supersonic transport and validated the concept numerically and experimentally, at scale and with a Reynolds number corresponding to previous wind tunnel tests: model length $L = 0.33$ m or $L = 0.74$ m, Mach

number $M = 2$, and unit Reynolds number $Re_{unit} = 12.3$ million/m [26–28].



Fig.1 Conceptual image of the small supersonic civil transport *QSST* [29].

This study was conducted to design the NLF fuselage nose at a scale and with a Reynolds number corresponding to the small supersonic civil transport, expanding the obtained NLF concept. The transport examined here is a small supersonic civil transport, *QSST*, which has been designed conceptually at JAXA [29]. However, the results are introduced herein not only for *QSST*, but also for a Sears–Haack body (SH), which is well known as an axisymmetric shape with minimum wave drag. It is useful to validate our NLF concept because of its simple shape. The respective resultant shapes are abbreviated to an SH-based case and to a *QSST*-based case.

2 Small Supersonic Civil Transport *QSST*

The technical objectives for *QSST*, the small supersonic civil transport designed conceptually at JAXA, are the following [29].

- Attain supersonic flight over land by sonic boom reduction (half the sonic boom strength of the *Concorde*)
- Meet noise level standards applied to current subsonic passenger transport during takeoff and landing (complying with ICAO Chap. 4)

- Reduce fuel usage by reducing aerodynamic drag, thereby lengthening the cruising distance (cruising lift–drag ratio higher than 8.0)
- Reduce structural weight to reduce fuel consumption and to lengthen the cruising distance (15% of the structural weight of the *Concorde*)

And the present design conditions of *QSST* are listed in Table 1.

Table 1. Design conditions of *QSST* [29].

Overall length	47.8 m
Breadth	23.6 m
Total height	7.3 m
Area of main wing	175 m ²
Aspect ratio	3.0
All-up weight	70 ton
Engine	15 ton twin-engine
Number of passengers	36–50
Cruising speed	Mach 1.6
Unit Reynolds number	6.45 million/m
Cruising distance	More than 3500 nm

3 Design of Natural Laminar Flow Fuselage Nose

Key knowledge for the design of the NLF fuselage nose, as obtained through the transition analysis for axisymmetric bodies [24, 25] and for the NLF fuselage nose [26–28] at the wind tunnel condition, is the following:

Cross-flow velocity component, which is normal to the streamline and leads 3-D boundary layer such as the side area of a nose-like shape to the early transition, is suppressed when the ratio of pressure gradients in azimuthal and axial directions at the side area is small. The pressure gradients in the azimuthal direction can be inferred from the adequate non-symmetric shape between upper and lower sides (i.e., the leeward and windward sides).

Therefore the NLF fuselage nose is described as a modification from the baseline shape using the Gaussian function. The radius distribution of the modified shape $R(x, \varphi)$ is

defined as the sum of a baseline $R_0(x, \varphi)$ and a modification $dR(x, \varphi)$, where x , y , z and φ respectively denote the axial, horizontal and vertical length from the nose tip and the azimuthal angle from the leeward symmetric plane.

$$R(x, \varphi) = R_0(x, \varphi) + dR(x, \varphi). \quad (1)$$

As described above, SH and the fuselage nose of QSST (specially abbreviated to QN in this report) are applied as baseline shapes. The radii distribution of SH is defined as shown below.

$$R_{SH}(x) = A_{SH} \left[\left(\frac{x}{L_{SH}} \right) \left\{ 1 - \left(\frac{x}{L_{SH}} \right) \right\} \right]^{(3/4)}. \quad (2)$$

Therein, $A_{SH} = 3.921198$ m and $L_{SH} = 48$ m. However, QN is designed based on the low-boom concept [29] and it cannot be described analytically. Furthermore, the NLF concept is applied to 6 m length from the nose tip for SH and 3 m length from the nose tip for QN because the transition location does not reach the entire fuselage. The cross-sectional area at the downstream end is fixed in the same way as that related to transport, to evaluate the drag consistently.

Moreover, a radius distribution of modification is defined as a product of azimuthal amplitude Φ_t , axial amplitude Ψ_t and weight function W_x as shown below.

$$dR(x, \varphi) = W_x(x) \times \sum_{t=1}^{t_{\infty}} \{ \Phi_t(\varphi) \times \Psi_t(x, x_{0t}(\varphi)) \}, \quad (3)$$

$$\Phi_t(\varphi) = \varepsilon_{0t} + 2\pi E_{0t} \times \exp \left[- \left(\frac{1}{2\lambda_t^2} \right) \{ \varphi - \varphi_{0t} \}^2 \right], \quad (4)$$

$$\Psi_t(x, x_{0t}(\varphi)) = 2\pi G_{0t} \times \exp \left[- \left(\frac{2\pi^2}{\kappa_t^2} \right) \left(\frac{\{ x - x_{0t}(\varphi) \}^2}{L^2} \right) \right], \quad (5)$$

$$\frac{x_{0t}(\varphi)}{L} = \frac{\tanh \left\{ \left(\varphi - \frac{\pi}{2} \right) \times H_{1t} \right\}}{H_{3t}} + H_{2t}, \quad (6)$$

$$W_x(x) = W_x(x, x_w, w_x) = \frac{W_1 \times W_2}{W_3}, \quad (7)$$

$$W_1 = \tanh \left\{ \left(\frac{w_x}{L} \right) (x - x_w) \right\} + \tanh \left\{ \left(\frac{w_x}{L} \right) x_w \right\}, \quad (8)$$

$$W_2 = \tanh \left\{ \left(\frac{w_x}{L} \right) (L - x - x_w) \right\} + \tanh \left\{ \left(\frac{w_x}{L} \right) x_w \right\}, \quad (9)$$

$$W_3 = \tanh \left\{ \left(\frac{w_x}{L} \right) \left(\frac{L}{2} - x_w \right) \right\} + \tanh \left\{ \left(\frac{w_x}{L} \right) x_w \right\}. \quad (10)$$

The NLF effect was evaluated using transition analysis for the parametrically modified fuselage nose.

4 Numerical Method for Transition Analysis

The transition location of the designed fuselage nose as described above is numerically predicted.

The mean laminar boundary layer flow at each condition was obtained from a Navier-Stokes calculation. Computations with an adiabatic wall boundary condition were performed at JAXA, using the 3-D, multi-block, structured-grid flow solver UPACS, which was developed by JAXA [30]. Computations were based on a typical grid, which is generated using an in-house grid generation code with about 9.5 million grid points for SH-based case or about 11.4 million grid points for QSST-based case in total. The convergence of computed solutions was confirmed via preliminary comparisons between solutions on different grid sizes [23-25, 31, 32].

The computed laminar mean flows were used as basic states for linear stability analysis.

The analysis were performed using the LSTAB code [23, 31, 32], which is based on linear stability theory for a 3-D compressible boundary layer. It was developed originally at JAXA. Parallel flow approximation is applied in this code. A partial set of results based on the e^N method is described below. The envelope method correlated the transition onset location with the logarithmic amplification ratio (i.e., N -factor) based on the most amplified fixed frequency disturbances. For each frequency, the N -factor distribution over the body surface was determined by integrating the maximum growth rate over all azimuthal wave numbers at each point along a selected set of trajectories. These trajectories were taken to be streamlines near the boundary layer edge in this paper. Transition location is predicted as the contour of $N=14$ according to the previous result of the supersonic flight test [33].

The validity of linear stability analysis, mean flow computation and number of grid points has been confirmed previously from the comparison between several other codes and grids [23-25, 31, 32].

5 Results

The results of numerical analysis are presented below. As described above, the SH-based case and QSST-based case are both illustrated.

5.1 SH-based Case

The most effective modification at the condition corresponding to the wind tunnel test was enlarged to the front half of the present fuselage nose and was applied to the Sears-Haack body. The boundary layer flow was analyzed under the condition of unit Reynolds number $Re_{unit} = 7.55$ million/m, corresponding to the preliminary design of *QSST* instead of the present design.

The modified shape (SHM) and the Sears-Haack body (SH) as its baseline shape are shown in Fig.2. The concept of this design is the minimization of pressure gradient in azimuthal direction in order to suppress the growth of cross-flow instability as mentioned above.

It might be readily apparent that the pressure distribution C_p of SHM, superimposed to Fig. 2(a) as a contour, is close to the axisymmetric distribution even it is set in the flow at non-zero incident, in contrast to the baseline shape (SH; Fig. 2(b)). This approximate axisymmetric property reduces the amplification of maximum cross-flow velocity component, the maximum of the velocity profile at the local location (Fig.3). At the black region near the tip and the downstream end, the computing accuracy of cross-flow velocity component is less-accurate.

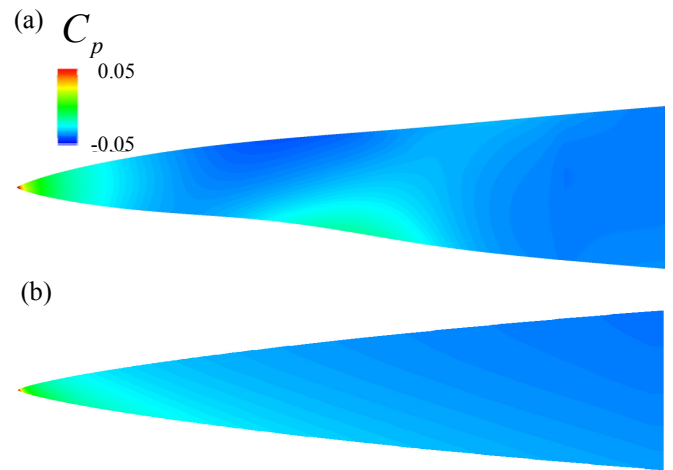


Fig.2 Distribution of pressure coefficient C_p on the surface; (a) modified shape (SHM) and (b) baseline shape (SH).

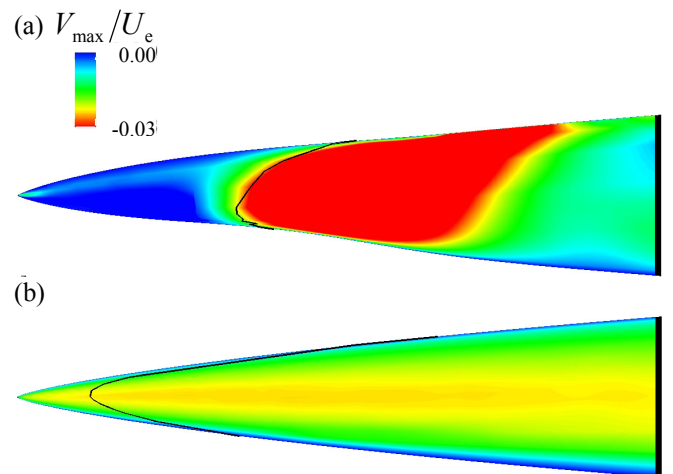


Fig.3 Cross-flow velocity component with the predicted transition location ($N=14$ line) on the surface; (a) modified shape (SHM) and (b) baseline shape (SH).

Results show that the transition front, which is predicted as the contour corresponding to $N=14$, moved further downstream 2 m from the nose tip. The delay from the baseline shape was about 1.3 m long. Moreover the transition Reynolds number $Re_{\tau}=15.2$ million was almost three times larger than that of the Sears-Haack body. The modified shape is confirmed as a more effective NLF shape than its baseline shape. Moreover, results emphasize that the transition Reynolds number was almost twice as large as the largest transition Reynolds number on the main wing of *NEXST-1*, which was obtained by the flight test [3, 4]. It is also twice as large as the predicted transition location on the model for wind tunnel test [28].

However, this modification requires the large increase of diameter in aft region. Then the resultant compression yields an increase of pressure drag C_{Dp} . Results show that the reduction of friction drag C_{Df} is less than the increase of C_{Dp} , at the aft part of modification (Fig. 4). This inadequacy encourages the confinement of modification not only in the meaning of the extent, but also of the strength.

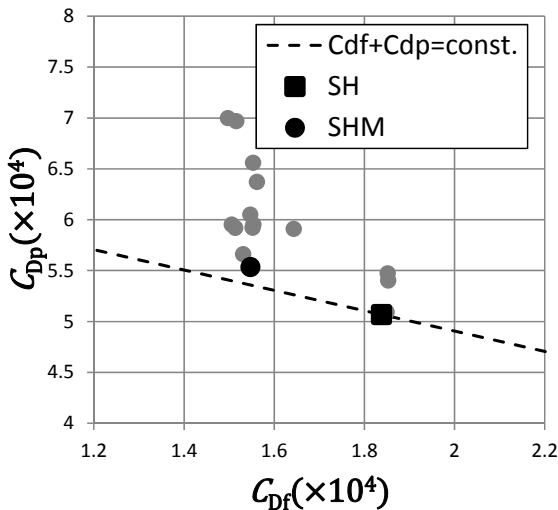


Fig.4 Drag coefficients.

5.2 QSST-based Case

Before the illustration of modified shape, the flow characteristics of baseline shape (QN) are

shown. The following analysis was performed under the condition of unit Reynolds number $Re_{unit} = 6.45$ million/m according to the present design conditions of *QSST*. The anti-axisymmetric shape is shown in Fig.5: panel (a) shows the side view; panel (b) portrays typical cross sections. This distinctive shape, especially that of windward side, is important for sonic-boom mitigation.

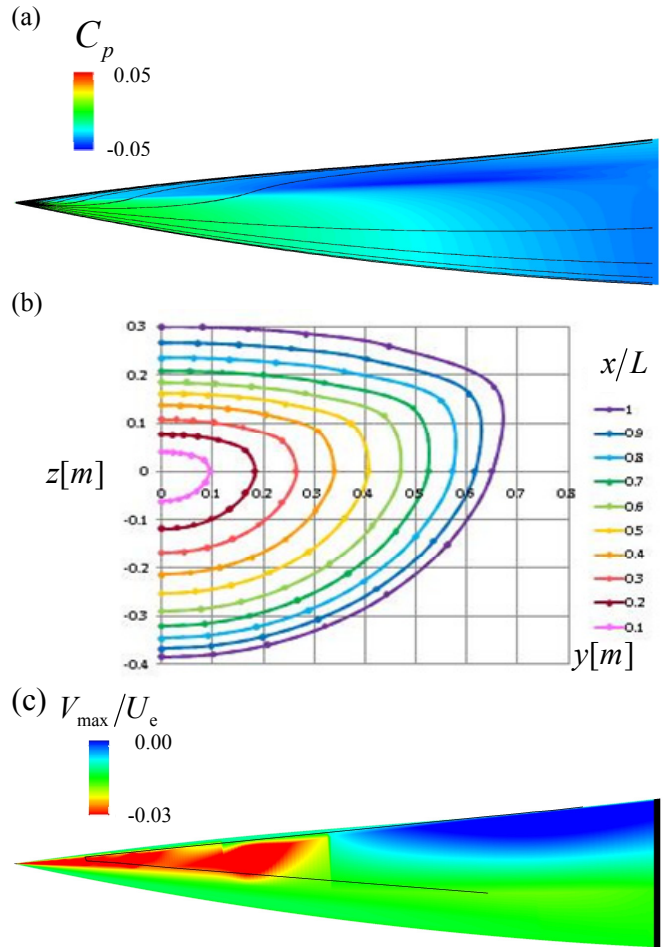


Fig.5 Flow characteristics of baseline shape (QN); (a) distribution of pressure coefficient C_p and streamlines on the side view, (b) cross sections, (c) cross-flow velocity component and predicted transition location ($N=14$ line).

The distribution of pressure coefficient C_p is also shown on the surface, superimposing the surface streamlines in Fig. 5(a). The difference of pressure coefficient between leeward and windward sides is apparent because of the flattened cross section (Fig. 5(b)). It yields the very high curvature of streamlines (Fig. 5(a))

and the corresponding large maximum cross-flow velocity component at the side (Fig.5(c)). As a result, a transition is predicted to occur at a location close to the tip. In contrast, the flow filed at the windward side just like a “wedge” allows the large extent of laminar boundary layer. The predicted transition location ($N=14$ line) moves more downstream from the downstream end which is 3 m long from the tip. Clearly, the opponent of the present study is the cross-flow component at the side area.

Then, following the results of SH-based case, confined modification, not only in the meaning of the extent but also of the strength, was applied at the side area for QN. That modification is shown in Fig.6. The modification forms a bump preventing flow from the windward side to the leeward side. Although the deformation is small, the large cross-flow velocity is markedly lower (Fig. 7) than that of its baseline shape (Fig. 5(c)).

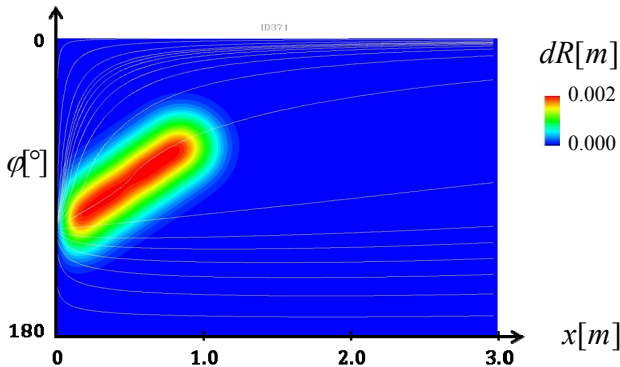


Fig.6 Contour of radii modification with surface streamlines of QNM.

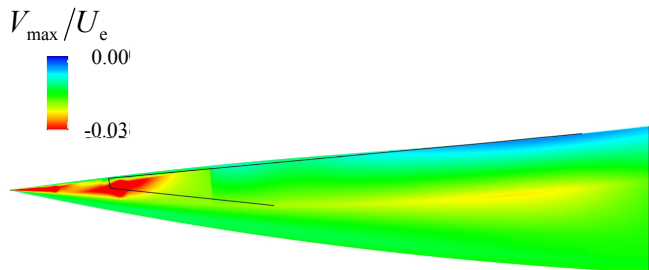


Fig.7 Contour of maximum cross-flow velocity component and the predicted transition location ($N=14$ line) of QNM.

Moreover the delay of predicted transition location ($N=14$) was confirmed (Fig.8). The friction drag was not compared because

estimation of the wetted-area from the discrete predicted transition location seems much less-accurate. However, the reduction of friction drag is naturally expected from decreased extent of large cross-flow area. Nevertheless, no increase of the pressure drag from its baseline shape was confirmed. Therefore, greater scope of the improvement of friction drag remains. Reduction of the total drag can be expected.

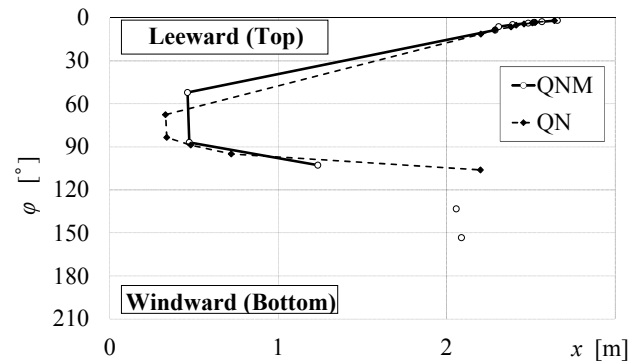


Fig.8 Comparison of the transition location predicted as $N=14$ between QNM and QN.

6 Concluding Remarks

A natural laminar flow fuselage nose is designed at scale and with a Reynolds number corresponding to the small supersonic civil transport *QSST* aimed at reducing friction drag.

The natural laminar flow effect was evaluated using transition analysis for the parametric modified fuselage nose from the baseline shape. Results show that the transition front, which is predicted as the contour corresponding to $N=14$, moved 2 m further downstream from the nose tip for SH-base case. It was almost three times larger than that of the baseline shape. On the other hand, for the *QSST*-base case, deformation was applied with a small extent preventing flow from the windward side to the leeward side. A decreasing extent of large cross-flow velocity and a resultant delay of transition front were observed

Acknowledgements

The authors thank Dr. K. Yoshida of JAXA and Prof. K. Matsushima of University of Toyama for their valuable advice. They also

acknowledge the support from Mr. T. Kawai, Ms. A. Tozuka and Mr. Y. Sasaki, who are all former trainees of JAXA and graduates of Aoyama Gakuin University.

References

- [1] Honda M. and Yoshida, K., *ICAS 2012-1.2.1*, 2012
- [2] Naka, Y., *JAXA-RM-11-010E*, 2012.
- [3] Yoshida, K., et al., *ICAS 2010-2.8.2*, 2004.
- [4] Tokugawa, N., et al., *J. of Aircraft*, Vol. 45, pp.1495-1504, 2008.
- [5] Peltzer, I., et.al. *ICAS 2006-3.3.1*, 2006.
- [6] Anders, S. G. and Fischer, M. C., *NASA-TP-1999-209683*, 1999
- [7] Saric, W. S., et al., *AIAA Paper 2002-0147*, 2002.
- [8] Bechert, D.W., et.al., *J. Fluid Mech.*, Vol. 338, pp.59-87, 1997.
- [9] Collier, F., *ICAS 2010-1.6.1*, 2010.
- [10] König, J. and Hellstrom, T., *ICAS 2010-5.9.3*
- [11] Iuliano, E., et. al., *AIAA Paper 2009-1279*, 2009.
- [12] Sturdza, P., *AIAA Paper 2007-0685*, 2007.
- [13] Fujino, M., *ICAS 2004-1.7.2* 2004.
- [14] Lutz, T. and Wagner, S., *J. of Aircraft*, Vol. 35, pp.345-351, 1998.
- [15] Dodbele, S. S., et. al., *J. of Aircraft*, Vol. 24, pp.298-304, 1987
- [16] Dodbele, S. S., *J. of Aircraft*, Vol. 29, pp.343-347, 1992
- [17] Zedan, M.F., et. al. *J. of Aircraft*, Vol. 31, pp.279-287, 1994.
- [18] Dodbele, S. S., et. al., *NASA CP-3970*, 1986.
- [19] Vijgen, P. M. H. W. and Holmes, B. J., *NASA CP-2487*, 1987, p. 861.
- [20] King, R. A., *Exp. in Fluids*, Vol. 13, pp.305-314, 1992.
- [21] Dougherty, N. S. and Fisher, D. F., *AIAA paper 80-0154*, 1980.
- [22] Malik, M. and Balakumar, P., *AIAA Paper 92-5049*, 1992.
- [23] Ueda, Y., et. al., *ICAS 2004-2.8.2*, 2004.
- [24] Tokugawa, N., *AIAA paper 2012-3259*, 2012.
- [25] Choudhari, M., et al., *ICCFD7-2306*, 2012.
- [26] Tokugawa, N., et al., *JAXA-RR-13-008*, 2014.
- [27] Tokugawa, N., et al., submitted to *Koku-Uchu-Gijyutsu (Aerospace Technology Japan, the Japan Society for Aeronautical and Space Sciences)*.
- [28] Tokugawa, N., et al., to appear in *Transactions of the Japan Society for Aeronautical and Space Sciences, Aerospace Technology Japan*.
- [29] <http://www.aero.jaxa.jp/eng/research/frontier/sst/concept.html/>
- [30] Yamazaki, H., et al., *High Performance Computing, Lecture Notes in Computer Science*, Vol. 1940, pp. 182-190, 2000.
- [31] Yoshida, K., et.al., *JAXA-RR-08-007E*, 2010.
- [32] Yoshida, K., et.al., *JAXA-RR-12-009E*, 2013.
- [33] Joslin, R. D., *Ann. Rev. of Fluid Mech.*, Vol. 30, pp.1-29, 1998.

Copyright Statement

The authors confirm that they, and/or their company or organization, hold copyright on all of the original material included in this paper. The authors also confirm that they have obtained permission, from the copyright holder of any third party material included in this paper, to publish it as part of their paper. The authors confirm that they give permission, or have obtained permission from the copyright holder of this paper, for the publication and distribution of this paper as part of the ICAS 2014 proceedings or as individual off-prints from the proceedings.

Contact Author Email Address

mailto: tokugawa.naoko@jaxa.jp